Mitochondria-translocated phosphoglycerate kinase 1 functions as a protein kinase to coordinate glycolysis and TCA cycle in tumorigenesis

Xinjian Li[1], **Yuhui Jiang**[1,2], **Jill Meisenhelder**[3], **Weiwei Yang**[1], **David H. Hawke**[4], **Yanhua Zheng**[1], **Yan Xia**[1], **Kenneth Aldape**[4], **Jie He**[5], **Tony Hunter**[3], **Liwei Wang**[2], and **Zhimin Lu**[1,6,7,*]

[1]Brain Tumor Center and Department of Neuro-Oncology, The University of Texas MD Anderson Cancer Center, Houston, TX 77030, USA

[2]The Institute of Cell Metabolism and Disease, Shanghai Key Laboratory of Pancreatic Disease, Shanghai General Hospital, School of Medicine, Shanghai Jiaotong University, Shanghai, 200080, China

[3]Molecular and Cell Biology Laboratory, Salk Institute for Biological Studies, La Jolla, California 92037, USA

[4]Department of Pathology, The University of Texas MD Anderson Cancer Center, Houston, TX 77030, USA

[5]Laboratory of Thoracic Surgery, Cancer Institute and Hospital, Chinese Academy of Medical Sciences, Peking Union Medical College, Beijing, 10002, China

[6]Department of Molecular and Cellular Oncology, The University of Texas MD Anderson Cancer Center, Houston, TX 77030, USA

[7]Cancer Biology Program, The University of Texas Graduate School of Biomedical Sciences at Houston, Houston, TX 77030, USA

SUMMARY

It is unclear how the Warburg effect that exemplifies enhanced glycolysis in the cytosol is coordinated with suppressed mitochondrial pyruvate metabolism. We demonstrate here that hypoxia, EGFR activation, and expression of K-Ras G12V and B-Raf V600E induce mitochondrial translocation of phosphoglycerate kinase 1 (PGK1); this is mediated by ERK-dependent PGK1 S203 phosphorylation and subsequent PIN1-mediated *cis–trans* isomerization. Mitochondrial PGK1 acts as a protein kinase to phosphorylate pyruvate dehydrogenase kinase 1 (PDHK1) at T338, which activates PDHK1 to phosphorylate and inhibit the pyruvate dehydrogenase (PDH) complex. This reduces mitochondrial pyruvate utilization, suppresses reactive oxygen species production, increases lactate production, and promotes brain

*Correspondence: ; Email: zhiminlu@mdanderson.org

tumorigenesis. Furthermore, PGK1 S203 and PDHK1 T338 phosphorylation levels correlate with PDH S293 inactivating phosphorylation levels and poor prognosis in glioblastoma patients. This work highlights that PGK1 act as a protein kinase in coordinating glycolysis and the TCA cycle, which is instrumental in cancer metabolism and tumorigenesis.

Keywords

PGK1; PDHK1; PDH; mitochondria; phosphorylation; glycolysis; hypoxia; EGFR; K-Ras; B-Raf; tumorigenesis

INTRODUCTION

Most cancer cells even in the presence of ample oxygen predominantly produce energy by a high rate of glycolysis followed by lactic acid fermentation in the cytosol, rather than by oxidation of pyruvate in mitochondria as in most normal cells. This tumor-specific Warburg effect promotes tumor progression (Yang and Lu, 2013, 2015). Mitochondrial oxidative phosphorylation is regulated by the availability of oxygen and pyruvate, which are the terminal electron acceptor and the primary carbon source, respectively (Kim et al., 2006). Mitochondrial pyruvate metabolism is regulated by pyruvate dehydrogenase kinase (PDHK or PDK), which has 4 isoforms (PDHK1–4), and pyruvate dehydrogenase (PDH) (Roche and Hiromasa, 2007). PDHK1, whose expression is upregulated by hypoxia-inducible factor 1α (HIF1α), phosphorylates S293 of the PDH E1α subunit and inactivates the PDH complex that normally converts pyruvate to acetyl-coA and CO_2; this results in an inhibition of pyruvate metabolism and tricarboxylic acid (TCA) cycle–coupled electron transport and thus attenuation of mitochondrial respiration and ROS production (Kim et al., 2006; Papandreou et al., 2006). By excluding pyruvate from mitochondrial consumption, PDHK1 induction may promote glycolysis and increase the rate of conversion of pyruvate to lactate.

Phosphoglycerate kinase 1 (PGK1), the first ATP-generating enzyme in the glycolytic pathway, catalyzes the transfer of the high-energy phosphate from the 1-position of 1,3-diphosphoglycerate (1,3-BPG) to ADP, which leads to the generation of 3-phosphoglycerate (3-PG) and ATP (Bernstein and Hol, 1998). PGK1 expression is upregulated in human breast cancer (Zhang et al., 2005), pancreatic ductal adenocarcinoma (Hwang et al., 2006), radioresistant astrocytomas (Yan et al., 2012), and multidrug-resistant ovarian cancer cells (Duan et al., 2002) as well as in metastatic gastric cancer, colon cancer, and hepatocellular carcinoma cells (Ahmad et al., 2013; Ai et al., 2011; Zieker et al., 2010). In spite of its overexpression in many types of human cancer, the mechanisms underlying PGK1-promoted tumor development remain largely unclear.

In this report, we demonstrate that hypoxia, activation of EGFR, and expression of K-Ras G12V and B-Raf V600E induces ERK1/2 phosphorylation-dependent and PIN1 *cis–trans* isomerization-regulated mitochondrial translocation of PGK1. Mitochondrial PGK1, acting as a protein kinase, phosphorylates and activates PDHK1. This phosphorylation inhibits mitochondrial pyruvate metabolism and ROS production and enhances lactate production, thereby promoting tumor development.

RESULTS

Mitochondrial Translocation of PGK1 Is Mediated by ERK1/2-Dependent Phosphorylation

Metabolic enzymes execute their primary metabolic functions in cytosol and mitochondria. However, in response to extracellular stimuli, these enzymes, which include pyruvate kinase M2 (PKM2) and fumarase, possess functions that are not directly linked with their normal role in metabolism when their subcellular localization is altered (Jiang et al., 2015; Lu, 2012a, b; Yang et al., 2011). To determine whether PGK1 has subcellular compartment-dependent functions, we examined its cellular distribution upon hypoxia stimulation. IF analyses of U87 human glioblastoma (GBM) cells showed that hypoxia induced the perinuclear accumulation of PGK1 (Figure 1A), which was diminished by expression of short hairpin RNA (shRNA) targeting PGK1 (Figure S1A). Co-staining the cells with an anti-PGK1 antibody and MitoTracker, a fluorescent mitochondrial dye, showed that PGK1 co-localized with mitochondria under hypoxic conditions (Figure 1A). Cell fractionation analyses confirmed this and showed that hypoxia, which resulted in HIF1α accumulation (Figure S1B, left panel), induced about 12% of cytosolic PGK1 translocation to mitochondria (right panel). Prolonged hypoxic stimulation enhances HIF1α-depdendent PGK1 expression (Kim et al., 2006). However, siRNA depletion of HIF1α did not block hypoxia-induced mitochondrial translocation of PGK1, indicating that this process occurs independently of HIF1α (Figure S1C).

To determine whether PGK1 binds the outer membrane of mitochondria or translocates into them, we performed a proteinase K protection assay using mitochondria isolated from U87 and U251 GBM cells. Outer membrane marker TOM20, but not PGK1 and the intramitochondrial marker COX IV, was completely digested by proteinase K treatment, whereas upon Triton X-100 treatment, which solubilizes the outer and inner membranes of mitochondria, PGK1 and COX IV were accessible to proteinase K digestion (Figure S1D). In contrast, brief digitonin treatment, which damages the mitochondrial outer membrane, but not the inner membrane, had limited effect on the accessibility of mitochondrial PGK1 for proteinase K digestion (Figure S1E). In addition, upon mitochondrial subfractionation, PGK1 was co-isolated with the mitochondrial matrix protein MnSOD, but not with the inner membrane protein TIMM22 and intermembrane space protein cytochrome c (Figure 1B), indicating that PGK1 translocated into the mitochondrial matrix. These findings were further supported by immunogold transmission electron microscopy analyses (Figure 1C).

MAP kinase activation plays instrumental roles in hypoxia-induced cellular activities (Kronblad et al., 2005). Pretreatment of U87 cells with the JNK inhibitor SP600125, p38 inhibitor SB203580, MEK/ERK inhibitor U0126 blocked hypoxia-induced phosphorylation of c-Jun, MAPK/APK2 (a p38 substrate), and ERK1/2 respectively (Figure S1F). Immunoblotting analyses revealed that only MEK/ERK inhibition significantly reduced the hypoxia-induced mitochondrial translocation of PGK1 in U87 (Figure 1D) and U251 cells (Figure S1G). These results were supported by the results of IF analyses (Figure S1H). In addition, expression of the Flag-ERK2 K52R kinase-dead mutant blocked the hypoxia- (Figure S1I) and active HA-MEK1 Q56P mutant- (Figure S1J) induced mitochondrial translocation of PGK1. These results indicate that ERK1/2 activation is required and

sufficient for mitochondrial translocation of PGK1. In line with this conclusion, EGF stimulation (Figure 1E) or expression of oncogenic K-Ras G12V in BxPC-3 human pancreatic cancer cells (with no endogenous Ras mutation) and B-Raf V600E in CHL1 human melanoma cells (with no endogenous B-Raf mutation) (Flockhart et al., 2009; Yun et al., 2009) (Figure 1F) induced mitochondrial translocation of PGK1; notably, this translocation was blocked by U0126 treatment or ERK2 K52R expression.

We next performed co-immoprecipitation (IP) analyses and showed that ERK1/2 associated with PGK1 upon hypoxia stimulation (Figure S1K). An in vitro GST pull-down assay with purified recombinant active His-ERK2 and GST-PGK1 revealed that these two proteins interact directly (Figure S1L). MAP kinases contain a docking groove, which consists of the common docking (CD) domain and glutamate/aspartate (ED) sites (Lu and Xu, 2006). D316 and D319 in the CD domain and T157 and T158 in the ED sites of ERK2 are important for the recognition of its substrates (Lu and Xu, 2006). Co-IP assays revealed that endogenous PGK1 bound poorly to Flag-ERK2 D316/D319N and to Flag-ERK2 T157/T158E, and completely failed to bind an ERK2 mutant with combined CD domain/ED sites mutations (Figure S1M). These results indicate that PGK1 binds to the ERK2 docking groove.

ERK substrates often have a docking motif, which is characterized by a cluster of basic residues followed by an LXL motif (L represents leucine, but can also be isoleucine or valine; X represents any amino acid) (Yang et al., 2012b). Analysis of the PGK1 amino acid sequence with the Scansite program identified three putative ERK-binding sequences, 74-DKYSLEP<u>V</u>A<u>V</u>E-84, 170-HRAHSSM<u>V</u>G<u>V</u>N-180, and 273-AEKNG<u>V</u>K<u>I</u>T<u>L</u>P-283, which contain LXL motifs at V81/V83, V177/V179, and V278/I280/L282, respectively. Streptavidin pull-down of S-Flag-Biotin (SFB)–PGK1 proteins showed that only PGK1 V278A/I280R/L282R mutation markedly reduced binding to ERK1/2 (Figure S1N). These results indicate that the ERK2 docking groove binds to a docking motif in PGK1 at V278/I280/L282.

To determine whether PGK1 is a substrate of ERK1/2, we performed an in vitro kinase assay and showed that purified and active ERK2 phosphorylated bacterially purified PGK1 (Figure 1G). An analysis of PGK1 amino acid sequences revealed that PGK1 has a P-X-S/TP (where X can be any amino acid) ERK1/2 phosphorylation motif at S203. Mutation of S203 to Ala abolished ERK2-mediated PGK1 phosphorylation in vitro, as demonstrated by autoradiography and immunoblotting analyses using a specific anti-PGK1 pS203 antibody (Figure 1G). IF analysis showed that hypoxia stimulation resulted in accumulation of phosphorylated PGK1 S203 in mitochondria (Figure S2A). In addition, U0126 treatment and PGK1 S203A mutation (Figure 1H), but not SP600125 treatment (Figure S2B), abolished hypoxia-induced PGK1 S203 phosphorylation. In line with these findings, expression of ERK2 K52R mutant reduced active MEK1 Q56P-induced PGK1 S203 phosphorylation (Figure S2C). Notably, PGK1 S203A was resistant to hypoxia-induced mitochondrial translocation (Figures 1I and S2D). In contrast, a phosphorylation-mimic PGK1 S203D mutant was able to accumulate in mitochondria in the absence of hypoxia stimulation (Figures 1I and S2D), indicating that ERK1/2-mediated PGK1 S203 phosphorylation is required for mitochondrial translocation of PGK1.

Hypoxia results in EGFR activation ([Franovic et al., 2007]). Treatment with EGFR inhibitors AG1478 or gefitinib blocked hypoxia-induced EGFR phosphorylation (Figure S2E), ERK activation, and phosphorylation and mitochondrial translocation of PGK1 in U87 cells (Figure S2F). These results indicated that hypoxia induces ERK activation and mitochondrial translocation of PGK1 through activation of EGFR. Consistent with this finding, EGF-induced PGK1 S203 phosphorylation (Figure S2G) and S203 phosphorylation-dependent mitochondrial translocation of PGK1 (Figure S2H) were also observed. In addition, ERK2 K52R expression blocked K-Ras G12V- and B-Raf V600E-induced PGK1 S203 phosphorylation (Figure S2I). These findings indicated that hypoxia, activation of EGFR, and expression of oncogenic K-Ras and B-Raf all induce ERK-dependent phosphorylation and mitochondrial translocation of PGK1.

PIN1 Binds to and *cis–trans* Isomerizes Phosphorylated PGK1 for Mitochondrial Translocation of PGK1

The peptidyl-proline isomerase protein never in mitosis gene A interacting-1 (PIN1) recognizes phosphorylated pS/TP-peptide sequences and catalyzes their *cis-trans* isomerization. PIN1 can regulate subcellular redistribution of its substrates ([Lu and Hunter, 2014]). Co-IP analyses showed that hypoxia stimulation significantly increased the interaction between endogenous PIN1 and PGK1, which was blocked by U0126 treatment (Figure 2A). In addition, hypoxia stimulation induced strong binding of endogenous PGK1 to wild-type (WT) GST-PIN1 but not substrate-binding deficient GST-PIN1 WW domain mutant (Figure 2B). Unlike WT PGK1, PGK1 S203A failed to interact with GST-PIN1 (Figure 2C). The requirement of ERK1/2 activity for the interaction between PIN1 and PGK1 was confirmed by an in vitro binding assay, which showed that purified His-PGK1 bound to purified WT GST-PIN1 but not GST-PIN1 WW mutant, only in the presence of ERK2 and ATP (Figure 2D). In addition, purified PGK1 S203D, but not PGK1 S203A, was able to pull down either purified GST-PIN1 (Figure 2E) or endogenous PIN1 in U87 cells without hypoxia stimulation (Figure 2F).

To further examine whether the PGK1 pS203/P204 motif is a PIN1 substrate, we synthesized PGK1 oligopeptides containing phosphorylated or nonphosphorylated S203/P204. WT GST-PIN1, but not a catalytically inactive GST-PIN1 C113A mutant, isomerized the pS203/P204 peptide (Figure 2G, left panel) but not its nonphosphorylated counterpart (Figure 2G, right panel). In addition, GST-PIN1 isomerized the phosphorylation-mimic D203/P204 peptide, but at a lower efficiency than for the pS203/P204 peptide (Figure 2G, left panel). Consistent with this finding, His-tagged D203/P204 peptide bound to GST-PIN1 with a lower efficiency than the pS203/P204 peptide, but with a higher affinity than its nonphosphorylated counterpart (Figure S2J). Cell fraction analysis demonstrated that about 15% of PGK1 S203D translocated into the mitochondria (Figure S2K), and this rate was moderately increased by PIN1 overexpression (Figure S2K), reflecting the low efficiency of PGK1 S203D/P204 isomerization by PIN1. These results suggested that PIN1 specifically isomerizes the PGK1 pS203/P204 motif.

Next we showed that PIN1 deficiency completely blocked the hypoxia-induced mitochondrial translocation of PGK1, whereas this block was rescued by reconstituted

expression of WT PIN1 but not the PIN1 C113A catalytically-inactive mutant in *PIN1*^{−/−} mouse embryonic fibroblasts (Figure 2H). In addition, PIN1 deficiency blocked the mitochondrial translocation of the PGK1 S203D mutant, and the failure of PGK1 S203D translocation was rescued by reconstituted expression of WT PIN1 but not the PIN1 C113A mutant (Figure 2I). These results indicate that ERK1/2-mediated PGK1 phosphorylation leads to the binding of PIN1 to PGK1, which in turn leads to the *cis–trans* isomerization and subsequent mitochondrial translocation of PGK1.

PIN1 Regulates Binding of PGK1 to the TOM Complex

Nearly all mitochondrial pre-proteins are imported via the translocase of the outer membrane (TOM) complex containing three receptor proteins, TOM20, TOM70, and TOM22. TOM20 acts as a general import receptor and is the initial recognition site for substrates with presequences. Presequences, which are often located at the N-terminus of precursor proteins and form positively charged amphipathic α helices, are the classic type of mitochondrial targeting signals (Chacinska et al., 2009). A structural analysis of PGK1 revealed that it contains an α-helix (amino acids 38–53) at its N-terminus (Figure S2L) (Michelson et al., 1985). Co-IP analyses showed that hypoxia stimulation resulted in an interaction between PGK1 and TOM20 (Figure 3A). PIN1 deficiency abrogated this interaction, which was rescued by reconstituted expression of WT PIN1 but not the PIN1 C113A mutant (Figure 3B). In addition, incubation of purified WT GST-PGK1 or GST-PGK1 S203D mutant with purified His-TOM20 in the presence or absence of PIN1 showed that GST-PGK1 S203D, but not WT GST-PGK1, was able to bind to TOM20 only in the presence of PIN1 (Figure 3C). These results indicate that PIN1 is required for phosphorylated PGK1 to bind to the TOM complex.

To determine the presequence of PGK1 needed for its mitochondrial translocation, we expressed a C-terminally SFB-tagged PGK1 Δ1–57 protein lacking residues 1–57 containing the α-helix and found that this mutant failed to interact with TOM20 (Figure 3D). Combined mutation of positively charged R39 and K41, or K48 in the α-helix into Ala revaled that PGK1 R39/K41A, but not PGK1 K48A, abrogated the PGK1 and TOM20 interaction (Figure 3E), strongly suggesting that R39/K41 are key residues involved in PGK1 binding to the TOM complex. Notably, neither the PGK1 Δ1–57 mutant (Figure 3F) nor the PGK1 R39/K41A mutant (Figures 3G and 3H) was able to translocate into mitochondria upon hypoxia stimulation of U87 cells, as demonstrated by immunoblotting (Figures 3F and 3G) and IF (Figure 3H) analyses. Similar results for PGK1 R39/K41A were observed in U251 cells (Figure S2M). Given that PGK1 R39/K41 are not directly exposed on the surface of the PGK1 protein (Figure S2N), these results strongly suggest that PIN1-dependent *cis–trans* isomerization of the pS203P204 bond in PGK1 exposes the mitochondrial targeting signal containing R39/K41 residues for recognition of PGK1 by the TOM complex. To further support this conclusion, we incubated purified GST-PGK1 S203D mutant with or without purified PIN1 for isomerization, which was followed by IP with a specific anti-PGK1 antibody that recognizes 38-QRIKAA-43. Immunoblotting analyses with an anti-GST antibody showed that anti-PGK1 antibody against 38-QRIKAA-43 successfully recognized GST-PGK1 S203D only in the presence of PIN1 (Figure S2O). These results suggested that PIN1-regulated isomerization of PGK1 exposes the 38-QRIKAA-43 residues so that they

can be recognized by both the peptide-specific antibody and the TOM complex for mitochondrial translocation of PGK1.

Mitochondrial PGK1 Phosphorylates PDHK1

Hypoxia enhances the glycolytic pathway and results in pyruvate being converted into lactate rather than being used for mitochondrial oxidation (Semenza, 2010). As expected, hypoxia decreased the PDH complex–mediated conversion rate of ^{14}C-labeled pyruvate to ^{14}C-labeled CO_2 in isolated mitochondria (Figure 4A). Of note, PGK1 depletion significantly counteracted the suppression of pyruvate to CO_2 conversion observed with hypoxia, and this suppression was rescued by reconstituted expression of RNA interference-resistant (r) V5-tagged WT PGK1, but not of rPGK1 S203A or rPGK1 R39/K41A (Figures 4A and S3A). Similar results were obtained for hypoxia- or EGF-stimulated cells incubated with [1-^{14}C]-pyruvate (Figure S3B). These results indicate that mitochondrial PGK1 regulates the activity of the PDH complex.

In line with this finding, co-IP analyses showed that hypoxia induced an interaction between endogenous PGK1 and PDHK1 (Figure 4B). In addition, PDHK1, but not PDHK2, PDHK3, or PDHK4, interacted with endogenous PGK1 upon hypoxic stimulation (Figure S3C). Furthermore, purified PGK1 directly bound to purified PDHK1 in an in vitro binding assay (Figure 4C). These results indicated that hypoxia results in direct interaction between PGK1 and PDHK1.

PGK1-catalyzed conversion of 1,3-BPG to 3-PG and ATP is a reversible reaction (Bernstein and Hol, 1998) such that PGK1 can also utilize ATP as a phosphate donor. To test whether PGK1 might act as a protein kinase to phosphorylate PDHK1, we performed an in vitro phosphorylation assay by mixing highly purified recombinant PGK1 and PDHK1 (Figure S3D) in the presence of ATP (Figure 4D). Liquid chromatography-coupled Orbitrap mass spectrometry (LC-MS/MS) analyses of tryptic digests of PDHK1 showed that PGK1 phosphorylates PDHK1 at S337 or T338 (Figure 4D). Phosphoamino acid analysis showed that PGK1 phosphorylates PDHK1 predominantly at threonine (Figure S3E), suggesting that PDHK1 T338 is phosphorylated. In addition, WT PGK1, but not a PGK1 T378P kinase-dead mutant (Chiarelli et al., 2012), was able to phosphorylate WT PDHK1, but not PDHK1 T338A, which was detected by both autoradiography and an anti-phospho-PDHK1 T338 antibody (Figures 4E and S3F). In contrast, mutation of the adjacent PDHK1 S337A had no effect on PGK1-mediated PDHK1 phosphorylation (Figure S3G). This phosphorylation was abrogated by incubation with an excess amount of 3-PG (Figure S3H), suggesting that PDHK1 and 3-PG compete with each other for phosphorylation by PGK1.

To support that ATP is the physiological phosphate donor for PGK1-mediated PDHK1 phosphorylation, we mixed a mitochondrial lysate with purified PGK1 in the presence of exogenous ATPase. The presence of ATPase, which hydrolyzes mitochondrial ATP, abrogated PGK1-mediated PDHK1 T338 phosphorylation (Figure S3I). Given that the Km (0.56 ± 0.053 mM) of ATP for PGK1-dependent PDHK phosphorylation (Figure S3J) is much lower than the physiological mitochondrial concentrations of ATP in U87 and U251 cells, which range from 2.5 to 3.5 mM under normoxic and hypoxic conditions (Figure

S3K), these results suggests that PGK1 is able to efficiently phosphorylate PDHK1 in mitochondria utilizing ATP.

Depletion of phosphorylated PDHK1 from a mitochondrial extract using a PDHK1 pT338 antibody largely reduced the amount of PDHK1 in mitochondria, suggesting that the majority of mitochondrial PDHK1 was phosphorylated by PGK1 upon hypoxic stimulation (Figure S3L). Mitochondrial fraction analyses showed that both WT rPGK1 and rPGK1 T378P (Figure S3M) were able to translocate into mitochondria (Figure S3N). However, PGK1 depletion-blocked hypoxia-induced PDHK1 T338 phosphorylation was rescued by reconstituted expression of WT rPGK1 but not that of rPGK1 T378P (Figure S3O). In addition, expression of rPGK1 S203A, which had comparable glycolytic activity to its WT counterpart (Figure S3P), failed to induce PDHK1 T338 phosphorylation under hypoxic conditions (Figure 4F). PDHK1 is known to be phosphorylated at tyrosine residues by FOP2-fibroblast growth factor receptor (FGFR) 1, an oncogenic, soluble FGFR1 fusion protein (Hitosugi et al., 2011). Consistent with this previous finding, hypoxic stimulation did not alter PDHK1 Y243 phosphorylation (Figure S3Q). Given that the majority of mitochondrial PDHK1 was phosphorylated by PGK1, these results suggest that FGFR is not involved in the regulation of PDHK1 during hypoxia. These results indicated that PGK1 functions as a protein kinase and phosphorylates PDHK1 T338 in mitochondria under hypoxic condition.

PDHK1 phosphorylation by PGK1 activates PDHK1

To determine whether PGK1 regulates PDHK1 activity by phosphorylation, we examined the effect of PGK1 on PDHK1-phosphorylated PDH (E1α) by performing an in vitro protein kinase assay. We showed that PDHK1-dependent PDH S293 phosphorylation was significantly enhanced by purified WT PGK1 but not PGK1 T378P (Figure 5A). In addition, PDHK1 T338A, whose basal PDH phosphorylation activity was the same as WT PDHK1, did not exhibit PGK1-enhanced PDH phosphorylation (Figure 5A). These in vitro results were validated in U87 and U251 cells, which showed that PGK1 depletion blocked hypoxia-induced PDH phosphorylation and that this defect in phosphorylation was rescued by reconstituted expression of WT rPGK1 but not rPGK1 S203A (Figure 5B), rPGK1 T378P (Figure S4A), or rPGK1 R39/K41A (Figure S4B) that had comparable glycolytic activity to its WT counterpart (Figure S3O). Notably, cells expressing mitochondria translocation-defective rPGK1 R39/K41A did not exhibit increased PDH phosphorylation, although PDHK1 expression was dramatically enhanced by long-term hypoxic stimulation (Figure S4C). These results indicated that hypoxia-enhanced PDHK1 expression is not sufficient for full activation of PDHK1, which requires PGK1-dependent phosphorylation.

In line with these results, PDHK1 depletion or reconstituted expression of rPDHK1 T338A blocked hypoxia-induced PDH phosphorylation (Figure 5C). In addition, EGF treatment (Figure 5D) or expression of K-Ras G12V and B-Raf V600E (Figure 5E) resulted in enhanced phosphorylation of PDHK1 T338 and PDH S293, which was blocked by reconstituted expression of rPGK1 S203A (Figure 5D) or ERK2 K52R expression (Figure 5E). Furthermore, expression of dominant negative H-Ras N17 mutant blocked EGF-induced phosphorylation and motchondrial translocation of PGK1 and PDHK1

phosphorylation in EGFR-overexpressing 3Y1 rat fibroblasts (Figures S4D). Simialr inhibitory results were also observed by U0126 treatment of Panc1 pancreatic cancer cells with endogenously expressed K-Ras G12D mutant (Figures S4E).

To further validate our findings in vivo, we used CRISPR/Cas9 genome editing knock-in technology to replace endogenous PGK1 and PDHK1 with PGK1 S203A and PDHK1 T338A, respectively, in U87 cells (Figures S4F and S4G). Deficiency of PGK1 phosphorylation blocked short-time hypoxia- and/or EGFR activation-induced mitochondrial translocation of PGK1 and phosphorylation of PDHK1 T338 (Figure 5F). In addition, PGK1 S203 and PDHK1 T338 phosphorylation-dependent PDH S293 phosphorylation was also observed (Figures 5F and 5G). Notably, hypoxic stimulation of these PGK1 S203A knock-in cells, which enhanced expression of PGK1 S203A and PDHK1, resulted in a limited increase in PDH S293 phosphorylation when compared with stimulation of their parental cells (Figure S4H), further supporting that mitochondrial PGK1-dependent phosphorylation and activation of PDHK1 play major roles in PDH inhibition.

All together, these results indicated that hypoxia, activation of EGFR, and expression of K-Ras G12V and B-Raf V600E all result in PGK1-mediated phosphorylation of PDHK1, which enhances PDHK1 activity promoting PDH phosphorylation and inhibition.

PGK1-Mediated PDHK1 Phosphorylation Inhibits Mitochondrial Pyruvate Metabolism and Promotes Lactate Production

To determine the role of PGK1-dependent PDHK1 phosphorylation in regulating mitochondrial function, we mixed ^{14}C-labeled pyruvate with isolated mitochondria from hypoxia-stimulated U87 cells. We showed that PDHK1 depletion (Figure 5C, left panel) acting similarly to rPGK1 S203A expression (Figure 4A) significantly enhanced the conversion rate of $[1-^{14}C]$-labeled pyruvate to ^{14}C-labeled CO_2 and counteracted the suppression induced by hypoxia (Figure 6A). These effects were abrogated by reconstituted expression of WT rPDHK1. In contrast, rPDHK1 T338A expression was unable to suppress PDH-dependent pyruvate metabolism upon hypoxic stimulation (Figure 6A). Similar results were also obtained with hypoxia-stimulated U87 cells incubated with $[1-^{14}C]$-pyruvate (Figure S5A). In line with this finding, production of acetyl-CoA levels in mitochondria of U87 cells (Figure 6B) and U251 cells (Figure S5B) was suppressed by hypoxia, and this suppression was abrogated by depletion of PDHK1 and restored by reconstituted expression of WT rPDHK1, but not rPDHK1 T338A. Notably, hypoxic stimulation of U87 (Figure 6C) and U251 cells (Figure S5C) for 24 h enhanced ROS production, which was further increased by PDHK1 depletion. Reconstituted expression of WT rPDHK1 greatly suppressed ROS production compared to expression of rPDHK1 T338A (Figures 6C and S5C). Consistent with this finding, rPGK1 R39/K41A expression enhanced ROS production compared to expression of WT rPGK1 (Figure S5D). Furthermore, PGK1 depletion induced higher ROS production (Figure S5E) and mitochondrial membrane potential inhibition (Figure S5F), which was further enhanced by the addition of exogenous pyruvate. These results indicate that mitochondrial PGK1-mediated PDHK1 phosphorylation is instrumental in suppressing PDH-dependent pyruvate metabolism and mitochondrial ROS production under hypoxic condition.

Hypoxia enhances glycolysis ($^{Kim\ et\ al.,\ 2006}$). We detected increased cytosolic pyruvate levels (Figure 6D) and lactate production (Figure 6E) in U87 cells with short term-hypoxic stimulation, which did not alter PGK1 and PDHK1 expression (Figures 1D and 4F). Notably, this increase was blocked by depletion of PGK1 (left panels) or PDHK1 (right panels), which was restored by reconstituted expression of WT rPGK1 or rPDHK1 but not rPGK1 S203A or rPDHK1 T338A, respectively. In addition, reconstituted expression of rPGK1 S203D, which translocated into mitochondria for upregulation of PDHK1 activity, enhanced lactate production in contrast to reconstituted expression of WT rPGK1 (Figure S5G).

As expected, EGF stimulation inhibited the conversion of pyruvate to CO_2 in vivo (Figure S5H); suppressed oxygen consumption rate (OCR) (Figures 6F and S5I) and mitochondrial oxidation activity (Figure 6G); and increased extracellular acidification rate (ECAR) (Figures 6H and S5J). These effects were lacking in knock-in cells expressing PGK1 S203A or PDHK1 T338A, treatment of cells with dicholoroacetate (DCA) PDHK inhibitor, or depletion of PGK1 or PDHK1, which can be rescued by reconstituted expression of WT rPGK1 or WT rPDHK1, but not with rPGK1 S203A or rPDHK1 T338A mutants. Of note, a ^{3}H-glucose labeling experiment demonstrated that the EGF-enhanced glycolytic rate was not obviously affected by knock-in of expression of PGK1 S203A (Figure S5K). These results further supported that the PGK1 mutants do not oberviuosly alter the glycolytic activity of PGK1 and that mitochondrial PGK1-mediated PDHK1 phosphorylation increases the amount of cytosolic pyruvate and lactate by attenuating mitochondrial pyruvate metabolism.

Mitochondrial PGK1-Dependent PDHK1 Phosphorylation Promotes Cell Proliferation and Brain Tumorigenesis and Indicates a Poor Prognosis in GBM Patients

Mitochondrial PGK1-regulated cell metabolism and ROS production likely regulates cell proliferation. As expected, depletion of PGK1 or PDHK1 inhibited proliferation of U87 cells under hypoxic conditions (Figure S6A). Reconstituted expression of WT rPGK1 or rPDHK1 restored cell proliferation. In contrast, reconstituted expression of rPGK1 S203A and rPDHK1 T338A resulted in only partial rescue of these deleterious effects on cells. The cell proliferation defect was also observed in the cells with knock-in of expression of PGK1 S203A or PDHK1 T338A (Figure 7A). Treatment with N-acetyl-L-cysteine (NAC), a scavenger of free radicals, which reduced hypoxia-induced ROS production in mitochondria (Anastasiou et al., 2011, partially rescued growth inhibition of U87 cells induced by reconstituted expression of PGK1 R39/K41A mutant under hypoxic condition (Figure S6B). Under normoxic conditions, knock-in of expression of PGK1 S203A (Figure S6C) or PDHK1 T338A (Figure S6D) in U87 cells expressing active EGFRvIII mutant inhibited cell proliferation. In contrast, enhanced proliferation of cells expressing rPGK1 S203D was observed (Figure S6E). These results indicate that mitochondrial PGK1-dependent PDHK1 phosphorylation promotes cell proliferation under both hypoxic and normoxic conditions.

To investigate the mitochondrial function of PGK1 in brain tumor development, we intracranially injected athymic nude mice with U87 and GSC11 human primary GBM cells (Figure S6F) with or without depletion of PGK1 or PDHK1 and reconstituted expression of

their WT counterparts, rPGK1 S203A, rPGK1 S203D, rPGK1 R39/K41A, or rPDHK1 T338A. Dissection of the mice's brains revealed tumor growth in all of the animals injected with U87 cells (Figure 7B) or GSC11 cells (Figure S6G). In contrast, we detected no tumor growth or much smaller tumors in the brains of mice injected with the cells with depleted PGK1 or PDHK1, respectively. This tumor inhibition was abrogated by reconstituted expression of WT rPGK1 or rPDHK1 but not rPGK1 S203A, rPGK1 R39/K41A, or rPDHK1 T338, whereas rPGK1 S203D expression enhanced tumor growth (Figures 7B and S6G). Immunohistochemical (IHC) staining revealed strong phosphorylation of PGK1 S203 and PDHK1 T338 in U87 cells with reconstituted expression of their WT counterparts but not with reconstituted expression of rPGK1 S203A or rPDHK1 T338A (Figure S6H). Ki67 staining (Figure S6I) and a terminal deoxynucleotidyl transferase dUTP nick end labeling (TUNEL) assay (Figure S6J) of tumor specimens revealed rapid cellular proliferation and few apoptotic cells with reconstituted expression of WT rPGK1 or rPDHK1, in contrast to the slower cell proliferation and more apoptotic cells with reconstituted expression of rPGK1 S203A or rPDHK1 T338A. These results indicated that mitochondrial PGK1-dependent PDHK1 phosphorylation promotes brain tumorigenesis.

We next analyzed 50 human primary GBM specimens with specificity-validated antibodies (Figures S7A and S7B) (Kaplon et al., 2013). We showed that the phosphorylation levels of ERK1/2, PGK1 S203, PDHK1 T338, and PDH S293 were positively correlated with each other (Figure 7C). Quantification of the staining showed that these correlations were significant (Figure S7C). We compared the survival duration of the 50 patients, all of whom had received standard adjuvant radiotherapy after surgical resection of GBM followed by treatment with an alkylating agent (temozolomide in most cases), with tumor phosphorylation levels of PGK1 S203 and PDHK1 T338. The median survival duration was 201.3 and 192.4 weeks for patients whose tumors had low PGK1 S203 and PDHK1 T338 phosphorylation levels, respectively, and 90.2 and 82.9 weeks for those whose tumors had high phosphorylation levels of PGK1 S203 and PDHK1 T338, respectively. In a Cox multivariate model, the IHC scores of PGK1 S203 and PDHK1 T338 phosphorylation were independent predictors of GBM patient survival after adjustment for patient age, which is a relevant clinical covariate (Figure 7D). These results support a role for mitochondrial PGK1-dependent PDHK1 phosphorylation in the clinical behavior of human GBM and reveal a correlation among ERK1/2-dependent PGK1 phosphorylation, PGK1-dependent PDHK1 phosphorylation, and the clinical aggressiveness of GBM.

DISCUSSION

A tumor cell mass, developing initially in a vascular environment, can become severely hypoxic as a result of massive expansion distant from the vasculature (Guise et al., 2014). To survive this hypoxic stress and support growth, the tumor cells upregulate glycolysis and suppress pyruvate metabolism and oxidative phosphorylation in mitochondria so that pyruvate is converted to lactate in the cytoplasm and exported (Gatenby and Gillies, 2004). In normoxic conditions, activation of receptor tyrosine kinases or the presence of prevalent K-Ras and B-Raf mutations promotes the Warburg effect (Tani et al., 1985; Yaffe et al., 1997; Yang et al., 2012b). We reveal here an important mechanism underlying the coordinated regulation of glycolysis and the TCA cycle by subcellular compartment-specific

regulation of the glycolytic enzyme PGK1: hypoxic stress, EGFR activation, or expression of K-Ras G12V or B-Raf V600E results in ERK1/2-dependent phosphorylation of PGK1 at S203, leading to PIN1-dependent PGK1 *cis–trans* isomerization, binding of PGK1 to the TOM complex, and subsequently mitochondrial translocation of PGK1. In mitochondria, PGK1 directly interacts with and phosphorylates PDHK1 at T338. This phosphorylation enhances PDHK1 activity and PDHK1-mediated PDH phosphorylation, which results in the suppression of PDH-dependent pyruvate utilization and ROS production in mitochondria and increased cytosolic production of pyruvate and lactate. This metabolic alteration promotes cell proliferation and tumorigenesis (Figure 7E). The demonstration that PGK1 functions as a protein kinase highlights its dual roles as a glycolytic enzyme and protein kinase in integrated regulation of glycolysis and mitochondrial metabolism.

In the glycolytic pathway, PGK1 and puruvate kinase are the only two ATP-generating enzymes. PKM2 was reported as a protein kinase and utilizes the phosphate group from phosphoenolpyruvate but not ATP to phosphorylate histone H3 and STAT3, thereby regulating gene expression (Gao et al., 2012; Yang et al., 2012a). PKM2 was also shown to phosphorylate Bub3 and myosin light chain 2 to promote mitosis and cytokinesis, respectively (Jiang et al., 2014a; Jiang et al., 2014b). In addition, succinyl-5-aminoimidazole-4-carboxamide-1-ribose-5'-phosphate (SAICAR) binds to and enhances the protein kinase activity of PKM2 for phosphorylation of more than 100 proteins (Keller et al., 2014). Of note, these findings from multiple groups were debated by a recent report, which shows that protein phosphorylation spectrum PKM2-null lysates was not altered by recombinant PKM2 and suggests that previously observed PKM2 protein kinase activity might result from PKM2-associated protein kinases rather than PKM2 itself. However, PKM2, as one out of more than 500 protein kinases in mammalian cells, might not be able to alter autoradiography-generated phosphorylation spectrums of thousands of proteins in gels. Importantly, PKM2 protein kinase activity was demonstrated and validated by a more recent publication (Li et al., 2015), which showed that the yeast PKM2 homolog can directly phosphorylate histone H3 at T11 in vivo and in vitro. The current study shows that highly purified PGK1 with no obvious protein kinase contamination phosphorylated highly purified PDHK1 supporting that glycolytic enzymes can possess dual enzymatic activities, functioning both as metabolic enzymes and protein kinases.

Hypoxic cells increase glycolysis with suppressed cellular respiration. The suppressed cellular respiration was thought to result from the paucity of oxygen required for accepting electrons from the mitochondrial respiratory chain and from the inhibition of mitochondrial pyruvate metabolism and respiration, which can be regulated by several mechanisms, including HIF1α-upregulated PDHK1 expression (Kim et al., 2006). In our study, a deficiency in mitochondrial translocation of PGK1 induced by expression of PGK1 S203A, which had no effect on hypoxia-enhanced PGK1 and PDHK1 expression, largely reduced hypoxia-induced PDH phosphorylation. These results indicated that overexpression of PGK1 and PDHK1 by itself is not sufficient to maximize its cellular activity in mitochondria and that PGK1-mediated phosphorylation of PDHK1 and hypoxia-enhanced PDHK1 expression have a synergistic effect on regulating PDHK1 activity.

Although tumor cells can regulate glycolysis and mitochondria simultaneously via HIF-regulated expression of glycolytic genes and mitochondrial enzymes under hypoxic conditions, this regulation, which does not occur in normoxic conditions, is a chronic response and requires regulation of gene transcription. We found that activation of EGFR, K-Ras, and B-Raf under normoxic conditions or hypoxia stimulation induced an immediate or acute response in tumor cells by rapid mitochondrial translocation of PGK1, which led to inhibition of mitochondrial pyruvate metabolism and increased cytosolic glycolysis. Thus, our findings provide an instrumental concept of integrated regulation of glycolysis and the TCA cycle and provide a critical insight into the Warburg effect induced by prevalent oncogenes, such as EGFR, K-Ras, and B-Raf. Given that PGK1 expression is upregulated in human cancer and is associated with tumor metastasis and drug resistance (Ahmad et al., 2013; Duan et al., 2002), our findings—demonstrating that PGK1-dependent PDHK1 T338 phosphorylation promotes tumor cell proliferation and tumorigenesis and that the phosphorylation levels of PGK1 S203 and PDHK1 T338 correlate with glioblastoma prognosis—may provide a molecular basis for improved diagnosis and treatment of human cancer.

EXPERIMENTAL PROCEDURES

Measurement of PGK1 Activity

Purified recombinant WT or mutant PGK1 (10 ng) was incubated in 100 μl of reaction buffer (50 mM Tris-HCl pH 7.5, 5 mM $MgCl_2$, 5 mM ATP, 0.2 mM NADH, 10 mM 3-phosphoglycerate, and 10 U of GAPDH) at 25°C in 96-well plate and read at 339 nm in kinetic mode for 5 minutes.

Streptavidin and GST Pull-Down Assays

Streptavidin or glutathione agarose beads were incubated with cell lysate (1 mg/ml) or purified protein for 12 h. The beads were washed with the lysate buffer for three times.

TUNEL Assay

Mouse tumor tissues were sectioned with 5 μm thickness. Apoptotic cells were detected by using DeadEnd™ TUNEL Systems (Promega, Madison, WI) according to the manufacturer's instructions.

Supplementary Material

Refer to Web version on PubMed Central for supplementary material.

Acknowledgments

REFERENCES

Ahmad SS, Glatzle J, Bajaeifer K, Buhler S, Lehmann T, Konigsrainer I, Vollmer JP, Sipos B, Ahmad SS, Northoff H, et al. Phosphoglycerate kinase 1 as a promoter of metastasis in colon cancer. International journal of oncology. 2013

Ai J, Huang H, Lv X, Tang Z, Chen M, Chen T, Duan W, Sun H, Li Q, Tan R, et al. FLNA and PGK1 are two potential markers for progression in hepatocellular carcinoma. Cellular physiology and biochemistry : international journal of experimental cellular physiology, biochemistry, and pharmacology. 2011; 27:207–216.

Bernstein BE, Hol WG. Crystal structures of substrates and products bound to the phosphoglycerate kinase active site reveal the catalytic mechanism. Biochemistry. 1998; 37:4429–4436. [PubMed: 9521762]

Chacinska A, Koehler CM, Milenkovic D, Lithgow T, Pfanner N. Importing mitochondrial proteins: machineries and mechanisms. Cell. 2009; 138:628–644. [PubMed: 19703392]

Chiarelli LR, Morera SM, Bianchi P, Fermo E, Zanella A, Galizzi A, Valentini G. Molecular insights on pathogenic effects of mutations causing phosphoglycerate kinase deficiency. PloS one. 2012; 7:e32065. [PubMed: 22348148]

Duan Z, Lamendola DE, Yusuf RZ, Penson RT, Preffer FI, Seiden MV. Overexpression of human phosphoglycerate kinase 1 (PGK1) induces a multidrug resistance phenotype. Anticancer research. 2002; 22:1933–1941. [PubMed: 12174867]

Flockhart RJ, Armstrong JL, Reynolds NJ, Lovat PE. NFAT signalling is a novel target of oncogenic BRAF in metastatic melanoma. British journal of cancer. 2009; 101:1448–1455. [PubMed: 19724275]

Franovic A, Gunaratnam L, Smith K, Robert I, Patten D, Lee S. Translational upregulation of the EGFR by tumor hypoxia provides a nonmutational explanation for its overexpression in human cancer. Proceedings of the National Academy of Sciences of the United States of America. 2007; 104:13092–13097. [PubMed: 17670948]

Gao X, Wang H, Yang JJ, Liu X, Liu ZR. Pyruvate kinase M2 regulates gene transcription by acting as a protein kinase. Molecular cell. 2012; 45:598–609. [PubMed: 22306293]

Gatenby RA, Gillies RJ. Why do cancers have high aerobic glycolysis? Nature reviews. Cancer. 2004; 4:891–899. [PubMed: 15516961]

Guise CP, Mowday AM, Ashoorzadeh A, Yuan R, Lin WH, Wu DH, Smaill JB, Patterson AV, Ding K. Bioreductive prodrugs as cancer therapeutics: targeting tumor hypoxia. Chinese journal of cancer. 2014; 33:80–86. [PubMed: 23845143]

Hitosugi T, Fan J, Chung TW, Lythgoe K, Wang X, Xie J, Ge Q, Gu TL, Polakiewicz RD, Roesel JL, et al. Tyrosine phosphorylation of mitochondrial pyruvate dehydrogenase kinase 1 is important for cancer metabolism. Molecular cell. 2011; 44:864–877. [PubMed: 22195962]

Hwang TL, Liang Y, Chien KY, Yu JS. Overexpression and elevated serum levels of phosphoglycerate kinase 1 in pancreatic ductal adenocarcinoma. Proteomics. 2006; 6:2259–2272. [PubMed: 16493704]

Jiang Y, Li X, Yang W, Hawke DH, Zheng Y, Xia Y, Aldape K, Wei C, Guo F, Chen Y, et al. PKM2 Regulates Chromosome Segregation and Mitosis Progression of Tumor Cells. Molecular cell. 2014a; 53:75–87. [PubMed: 24316223]

Jiang Y, Qian X, Shen J, Wang Y, Li X, Liu R, Xia Y, Chen Q, Peng G, Lin SY, et al. Local generation of fumarate promotes DNA repair through inhibition of histone H3 demethylation. Nature cell biology. 2015; 17:1158–1168. [PubMed: 26237645]

Jiang Y, Wang Y, Wang T, Hawke DH, Zheng Y, Li X, Zhou Q, Majumder S, Bi E, Liu DX, et al. PKM2 phosphorylates MLC2 and regulates cytokinesis of tumour cells. Nature communications. 2014b; 5:5566.

Kaplon J, Zheng L, Meissl K, Chaneton B, Selivanov VA, Mackay G, van der Burg SH, Verdegaal EM, Cascante M, Shlomi T, et al. A key role for mitochondrial gatekeeper pyruvate dehydrogenase in oncogene-induced senescence. Nature. 2013; 498:109–112. [PubMed: 23685455]

Keller KE, Doctor ZM, Dwyer ZW, Lee YS. SAICAR induces protein kinase activity of PKM2 that is necessary for sustained proliferative signaling of cancer cells. Molecular cell. 2014; 53:700–709. [PubMed: 24606918]

Kim JW, Tchernyshyov I, Semenza GL, Dang CV. HIF-1-mediated expression of pyruvate dehydrogenase kinase: a metabolic switch required for cellular adaptation to hypoxia. Cell metabolism. 2006; 3:177–185. [PubMed: 16517405]

Kronblad A, Hedenfalk I, Nilsson E, Pahlman S, Landberg G. ERK1/2 inhibition increases antiestrogen treatment efficacy by interfering with hypoxia-induced downregulation of ERalpha: a combination therapy potentially targeting hypoxic and dormant tumor cells. Oncogene. 2005; 24:6835–6841. [PubMed: 16007158]

Li S, Swanson SK, Gogol M, Florens L, Washburn MP, Workman JL, Suganuma T. Serine and SAM Responsive Complex SESAME Regulates Histone Modification Crosstalk by Sensing Cellular Metabolism. Molecular cell. 2015; 60:408–421. [PubMed: 26527276]

Lu Z. Nonmetabolic functions of pyruvate kinase isoform M2 in controlling cell cycle progression and tumorigenesis. Chinese journal of cancer. 2012a; 31:5–7. [PubMed: 22200182]

Lu Z. PKM2 functions as a histone kinase. Cell Cycle. 2012b; 11:4101–4102. [PubMed: 23070542]

Lu Z, Hunter T. Prolyl isomerase Pin1 in cancer. Cell research. 2014; 24:1033–1049. [PubMed: 25124924]

Lu Z, Xu S. ERK1/2 MAP kinases in cell survival and apoptosis. IUBMB life. 2006; 58:621–631. [PubMed: 17085381]

Michelson AM, Blake CC, Evans ST, Orkin SH. Structure of the human phosphoglycerate kinase gene and the intron-mediated evolution and dispersal of the nucleotide-binding domain. Proceedings of the National Academy of Sciences of the United States of America. 1985; 82:6965–6969. [PubMed: 2995995]

Papandreou I, Cairns RA, Fontana L, Lim AL, Denko NC. HIF-1 mediates adaptation to hypoxia by actively downregulating mitochondrial oxygen consumption. Cell metabolism. 2006; 3:187–197. [PubMed: 16517406]

Roche TE, Hiromasa Y. Pyruvate dehydrogenase kinase regulatory mechanisms and inhibition in treating diabetes, heart ischemia, and cancer. Cellular and molecular life sciences : CMLS. 2007; 64:830–849. [PubMed: 17310282]

Semenza GL. HIF-1: upstream and downstream of cancer metabolism. Current opinion in genetics & development. 2010; 20:51–56. [PubMed: 19942427]

Tani K, Singer-Sam J, Munns M, Yoshida A. Molecular cloning and structure of an autosomal processed gene for human phosphoglycerate kinase. Gene. 1985; 35:11–18. [PubMed: 3839763]

Yaffe MB, Schutkowski M, Shen M, Zhou XZ, Stukenberg PT, Rahfeld JU, Xu J, Kuang J, Kirschner MW, Fischer G, et al. Sequence-specific and phosphorylation-dependent proline isomerization: a potential mitotic regulatory mechanism. Science. 1997; 278:1957–1960. [PubMed: 9395400]

Yan H, Yang K, Xiao H, Zou YJ, Zhang WB, Liu HY. Over-expression of cofilin-1 and phosphoglycerate kinase 1 in astrocytomas involved in pathogenesis of radioresistance. CNS neuroscience & therapeutics. 2012; 18:729–736. [PubMed: 22742733]

Yang W, Lu Z. Regulation and function of pyruvate kinase M2 in cancer. Cancer letters. 2013; 339:153–158. [PubMed: 23791887]

Yang W, Lu Z. Pyruvate kinase M2 at a glance. Journal of cell science. 2015; 128:1655–1660. [PubMed: 25770102]

Yang W, Xia Y, Hawke D, Li X, Liang J, Xing D, Aldape K, Hunter T, Alfred Yung WK, Lu Z. PKM2 phosphorylates histone H3 and promotes gene transcription and tumorigenesis. Cell. 2012a; 150:685–696. [PubMed: 22901803]

Yang W, Xia Y, Ji H, Zheng Y, Liang J, Huang W, Gao X, Aldape K, Lu Z. Nuclear PKM2 regulates beta-catenin transactivation upon EGFR activation. Nature. 2011; 480:118–122. [PubMed: 22056988]

Yang W, Zheng Y, Xia Y, Ji H, Chen X, Guo F, Lyssiotis CA, Aldape K, Cantley LC, Lu Z. ERK1/2-dependent phosphorylation and nuclear translocation of PKM2 promotes the Warburg effect. Nature cell biology. 2012b; 14:1295–1304. [PubMed: 23178880]

Yun J, Rago C, Cheong I, Pagliarini R, Angenendt P, Rajagopalan H, Schmidt K, Willson JK, Markowitz S, Zhou S, et al. Glucose deprivation contributes to the development of KRAS pathway mutations in tumor cells. Science. 2009; 325:1555–1559. [PubMed: 19661383]

Zhang D, Tai LK, Wong LL, Chiu LL, Sethi SK, Koay ES. Proteomic study reveals that proteins involved in metabolic and detoxification pathways are highly expressed in HER-2/neu-positive breast cancer. Molecular & cellular proteomics : MCP. 2005; 4:1686–1696. [PubMed: 16048908]

Zieker D, Konigsrainer I, Tritschler I, Loffler M, Beckert S, Traub F, Nieselt K, Buhler S, Weller M, Gaedcke J, et al. Phosphoglycerate kinase 1 a promoting enzyme for peritoneal dissemination in gastric cancer. International journal of cancer. Journal international du cancer. 2010; 126:1513–1520. [PubMed: 19688824]
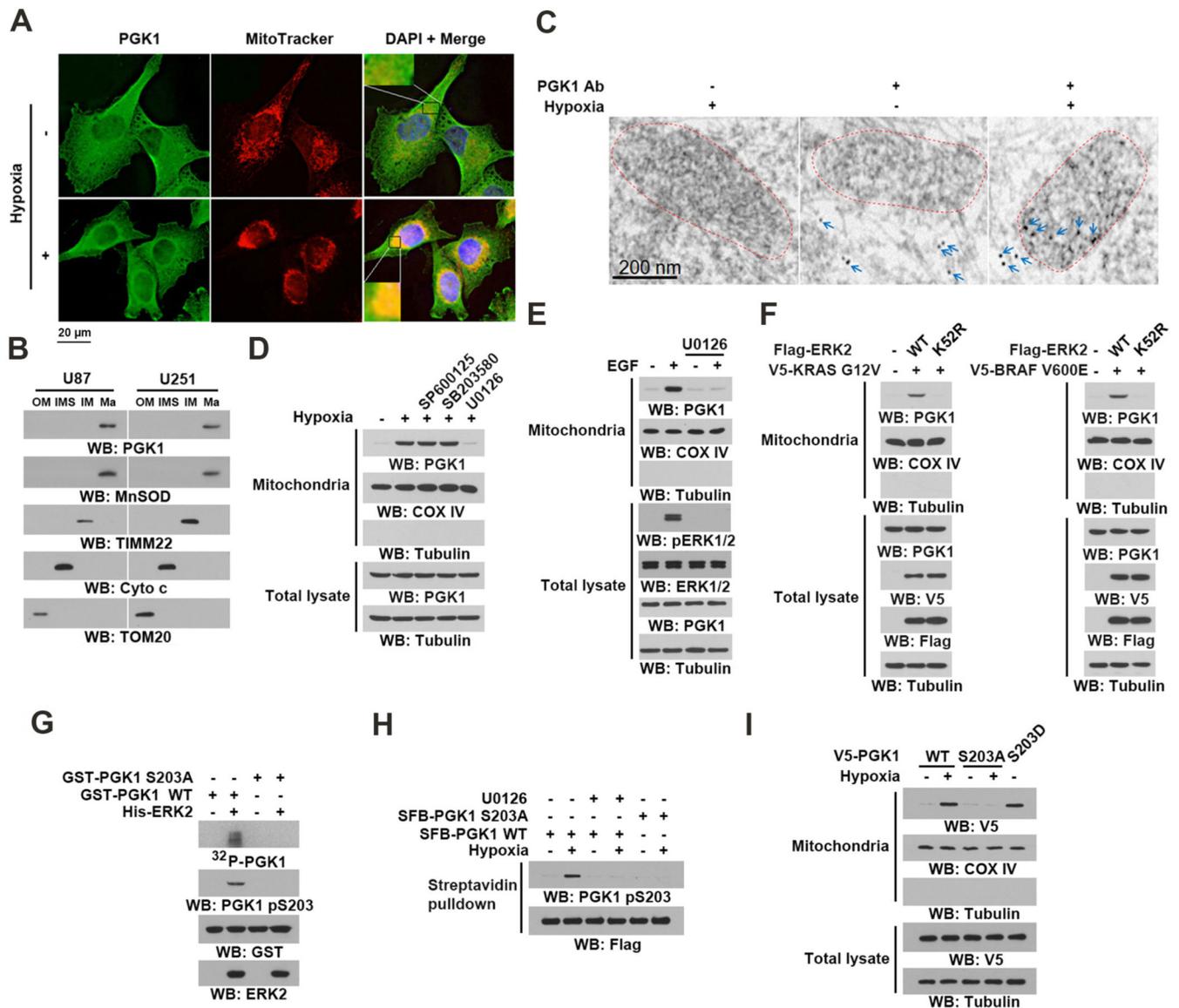
Figure 1. Mitochondrial Translocation of PGK1 Is Mediated by ERK1/2-Dependent Phosphorylation

(B, D–I), Immunoblotting and IP analyses were carried out using antibodies against the indicated proteins.

(A) U87 cells were stimulated with or without hypoxia for 6 h and stained with an anti-PGK1 antibody, MitoTracker, and DAPI.

(B) U87 and U251 cells were stimulated with hypoxia for 6 h. Proteins from mitochondrial outer membrane (OM), intermembrane space (IMS), inner membrane (IM), and matrix (Ma) were isolated.

(C) U87 cells were stimulated with or without hypoxia for 6 h. Electron microscopic immunogold analysis with anti-PGK1 antibody was performed. Arrows indicate representative staining of mitochondrial PGK1. Dashed circles indicate mitochondria.

(D) Mitochondria fractions and total cell lysates were prepared from U87 cells pretreated with SP600125 (25 μM), SB203580 (10 μM), or U0126 (20 μM) for 30 min before being treated with hypoxia for 6 h. Cytosolic tubulin was used as a control.

(E) EGFR-overxpressed U87 (U87/EGFR) cells pretreated with U0126 (20 μM) for 30 min were stimulated with or without EGF (100 ng/ml) for 6 h. Mitochondria fractions and total cell lysates were prepared.

(F) V5-KRAS G12V and the indicated Flag-ERK2 proteins were stably expressed in BxPC-3 cells (left panel). V5-BRAF V600E and the indicated Flag-ERK2 proteins were stably expressed in CHL1 cells (right panel). Mitochondria fractions and total cell lysates were prepared.

(G) In vitro kinase assays were carried out by mixing purified active ERK2 with purified WT GST-PGK1 or GST-PGK1 S203A in the presence of [γ-^{32}P]ATP. The reaction mixture was separated for autoradiography and immunoblotting analyses.

(H) U87 cells expressing the indicated SFB-PGK1 proteins were pretreated with or without U0126 (20 μM) for 30 min before hypoxic stimulation for 6 h. Streptavidin agarose beads were used to pull down SFB-tagged proteins.

(I) U87 cells expressing the indicated V5-tagged PGK1 proteins were treated with or without hypoxia for 6 h. Mitochondria fractions and total cell lysates were prepared.
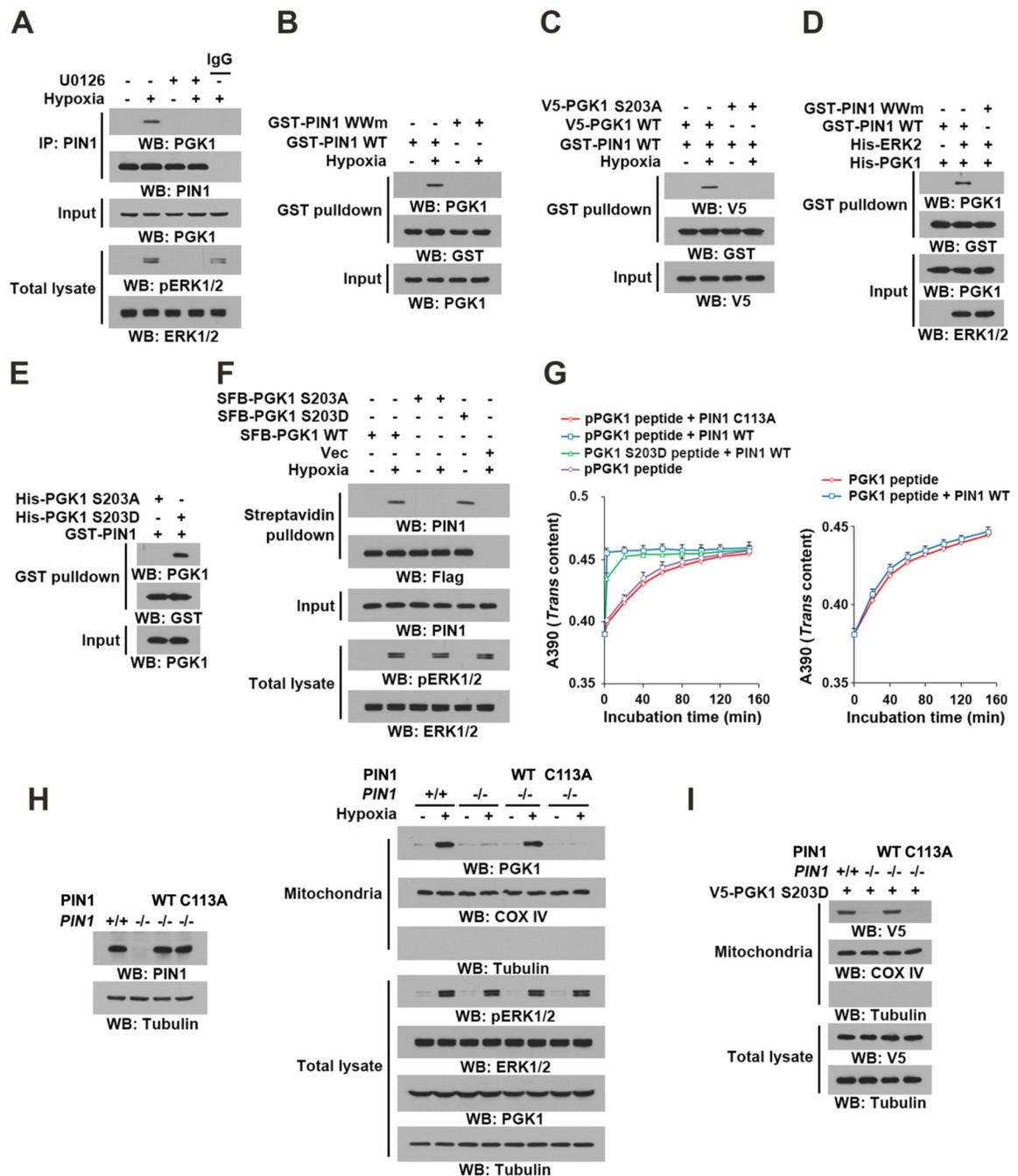
See also Figures S1 and S2.

Figure 2. PIN1 Binds to and *cis–trans* Isomerizes Phosphorylated PGK1 for Mitochondrial Translocation of PGK1

(A–F, H–I) Immunoblotting and IP analyses were carried out using antibodies against the indicated proteins.

(A) U87 cells were pretreated with or without U0126 (20 μM) for 30 min before hypoxic stimulation for 6 h.

(B) U87 cells were treated with or without hypoxic stimulation for 6 h. A GST pull-down assay with the indicted GST-proteins was performed. GST-PIN1 WWm: GST-PIN1 WW mutant.

(C) U87 cells expressing the indicated PGK1 proteins were treated with or without hypoxic stimulation for 6 h. A GST pull-down assay with GST-PIN1 proteins was performed.

(D) An in vitro protein kinase assay was performed by mixing purified recombinant PGK1 with or without purified active His-ERK2, which was followed by a GST pull-down assay with the indicated GST-proteins.

(E) A GST pull-down assay was performed by mixing GST-PIN1 and the indicated purified recombinant PGK1 proteins.

(F) U87 cells expressing the indicated SFB-PGK1 proteins were treated with or without hypoxia for 6 h. A pull-down assay with streptavidin agarose beads was conducted.

(G) *cis–trans* isomerization assays were performed by mixing synthesized phosphorylated or nonphosphorylated oligopeptides of PGK1 containing the S203P204 motif or an oligopeptide of PGK1 containing the D203P204 motif with purified wild-type GST-PIN1 or GST-PIN1 C113A mutant. Data represent the means ± SD of three independent experiments.

(H) *PIN1*$^{-/-}$ cells were reconstituted to express the indicated PIN1 proteins (left panel). The total cell lysates and motochondrial fractions were prepared from the indicated cells treated with or without hypoxia for 6 h (right panel).

(I) V5–PGK1 S203D was expressed in *PIN1*$^{+/+}$ cells and *PIN1*$^{-/-}$ cells with or without reconstituted WT PIN1 or PIN1 C113A. Total cell lysates and mitochondrial fractions of the cells were prepared.
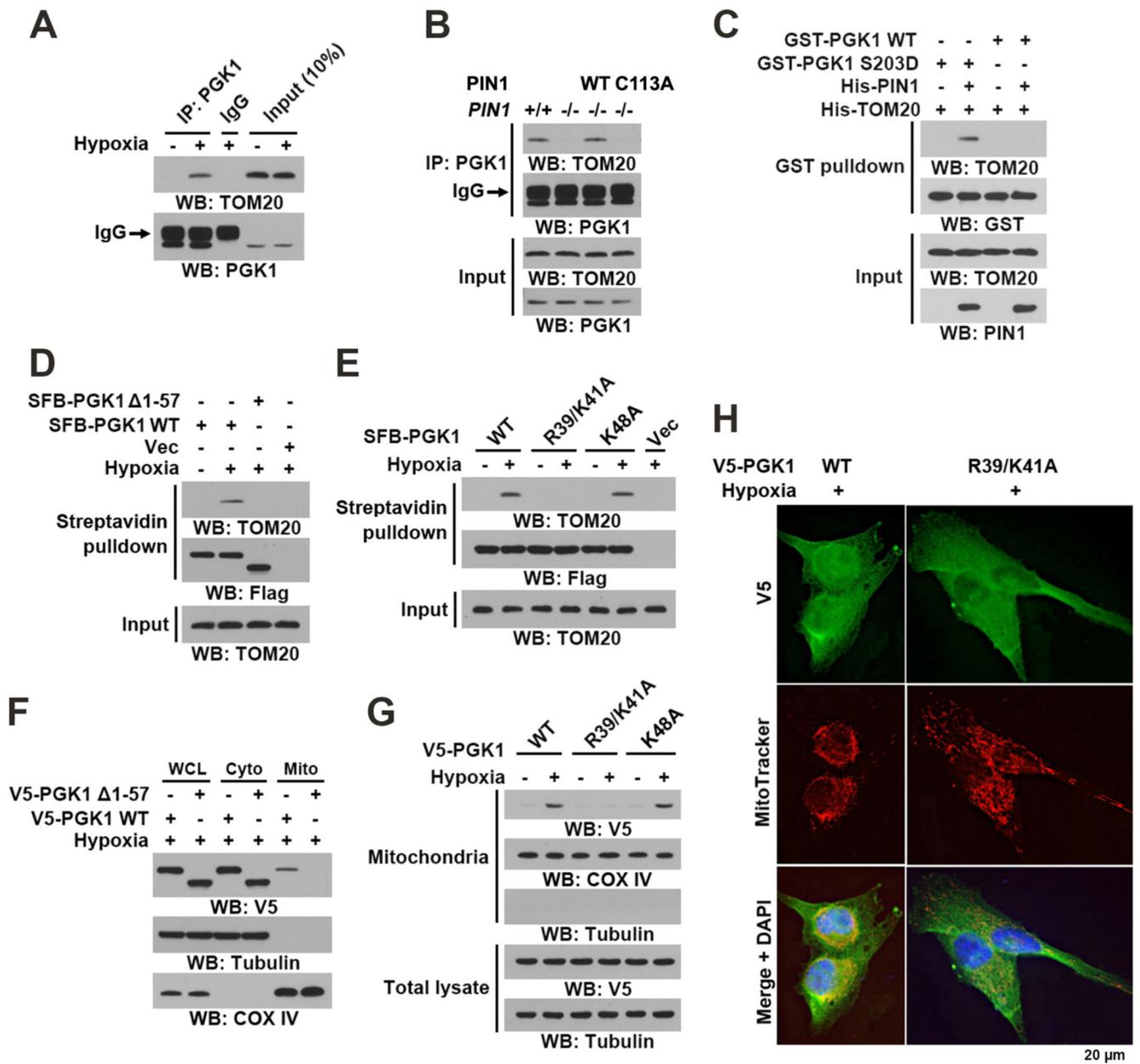
See also Figure S2.

Figure 3. PIN1 Regulates Binding of PGK1 to the TOM Complex

(A–G) Immunoblotting and IP analyses were carried out using antibodies against the indicated proteins.

(A) U87 cells were treated with or without hypoxia for 6 h. Total cell lysates were prepared.

(B) *PIN1*^{+/+} and the indicated *PIN1*^{−/−} cells were treated with hypoxia for 6 h.

(C) A GST pull-down assay was performed by mixing purified recombinant WT GST-PGK1 or GST-PGK1 S203D with His-TOM20 in the presence or absence of purified His-PIN1.

(D, E) U87 cells expressing the indicated SFB-PGK1 proteins were treated with or without hypoxia for 6 h. Streptavidin agarose beads were used to pull down SFB-tagged proteins.

(F, G) U87 cells expressing the indicated V5-tagged PGK1 proteins were treated with or without hypoxia for 6 h. Total cell lysate, cytosolic, and mitochondrial fractions were prepared.

(H) U87 cells expressing the indicated V5-PGK1 proteins were stimulated with or without hypoxia for 6 h and stained with an anti-V5 antibody, MitoTracker, and DAPI.
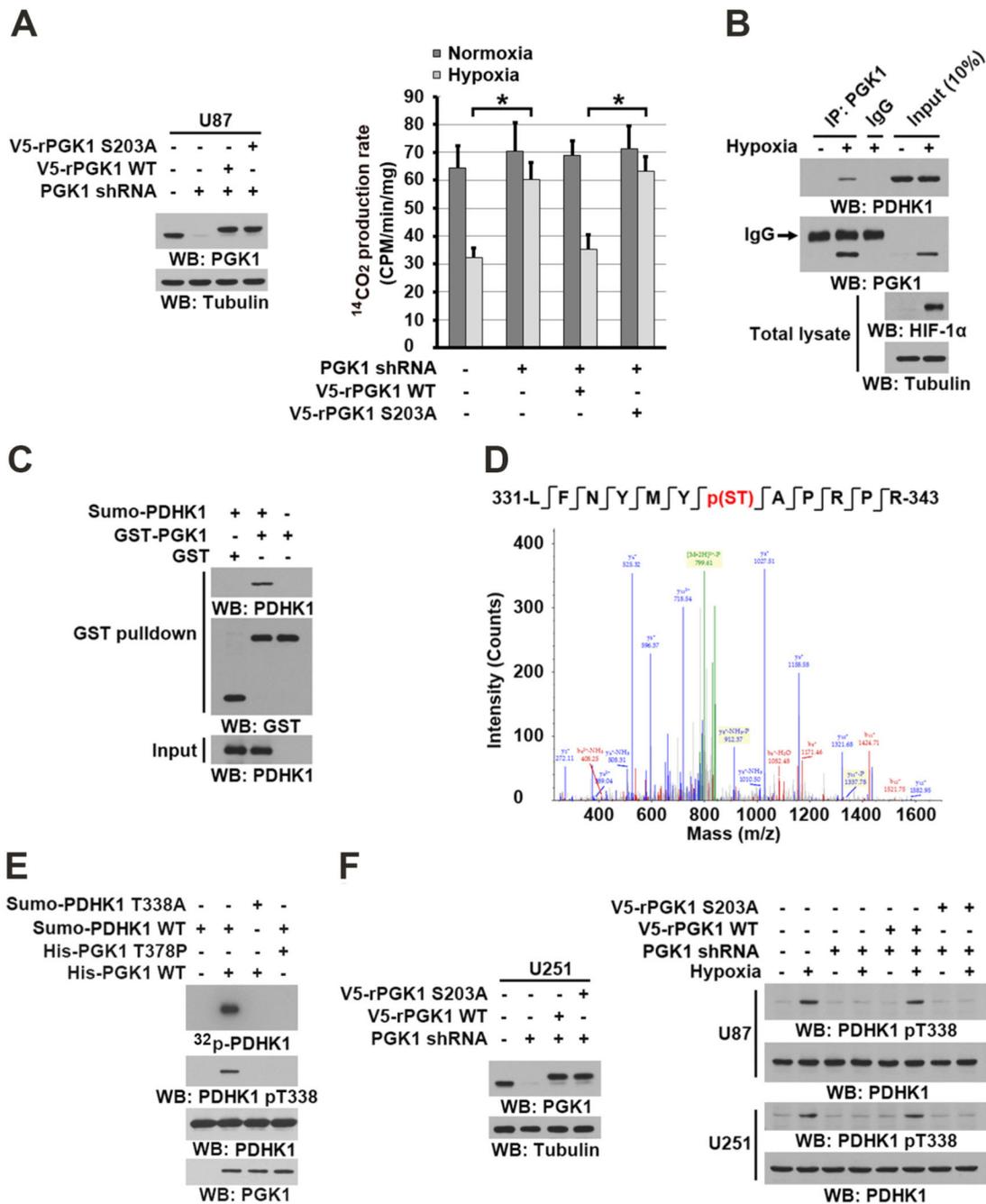
See also Figure S2.

Figure 4. Mitochondrial PGK1 Phosphorylates PDHK1

(A–C, E–F) Immunoblotting analyses were performed with the indicated antibodies.

(**A**) U87 cells with or without PGK1 shRNA and with or without reconstituted expression of WT rPGK1 or rPGK1 S203A were stimulated with or without hypoxia for 6 h. Isolated mitochondrial fractions were mixed with ^{14}C-labeled pyruvate, ADP, and malate under normoxic condtions. ^{14}C-CO$_2$ production rate was measured. Data represent the means ± SD of three independent experiments. *$p < 0.01$.

(B) U87 cells were stimulated with or without hypoxia for 6 h. Mitochondrial fractions of these cells were prepared. IP analyses with an anti-PGK1 antibody were performed.

(C) GST pull-down analyses were performed by mixing bacterially purified SUMO-PDHK1 proteins with purified GST or GST-PGK1.

(D) In vitro phosphorylation analyses were performed by mixing bacterially purified His-PGK1 and SUMO-PDHK1 in the presence of ATP. The mass spectrometry results of a fragment spectrum of a peptide at m/z 756.346 (mass error, ±4.2 ppm) matched to the doubly charged peptide 331-LFNYMYp(ST)APRPR-343, suggesting that S337 or T338 was phosphorylated. The Mascot score was 49, Expectation Value: 4.7E-004; the SEQUEST score for this match was Xcorr = 3.5.

(E) In vitro phosphorylation analyses with autoradiography were performed by mixing purified WT PGK1 or PGK1 T378P with purified WT PDHK1 or PDHK1 T338A in the presence of $[\gamma\text{-}^{32}P]$ATP.

(F) U251 and U87 cells with or without PGK1 shRNA and with or without reconstituted expression of WT rPGK1 or rPGK1 S203A were stimulated with or without hypoxia for 6 h. See also Figure S3.
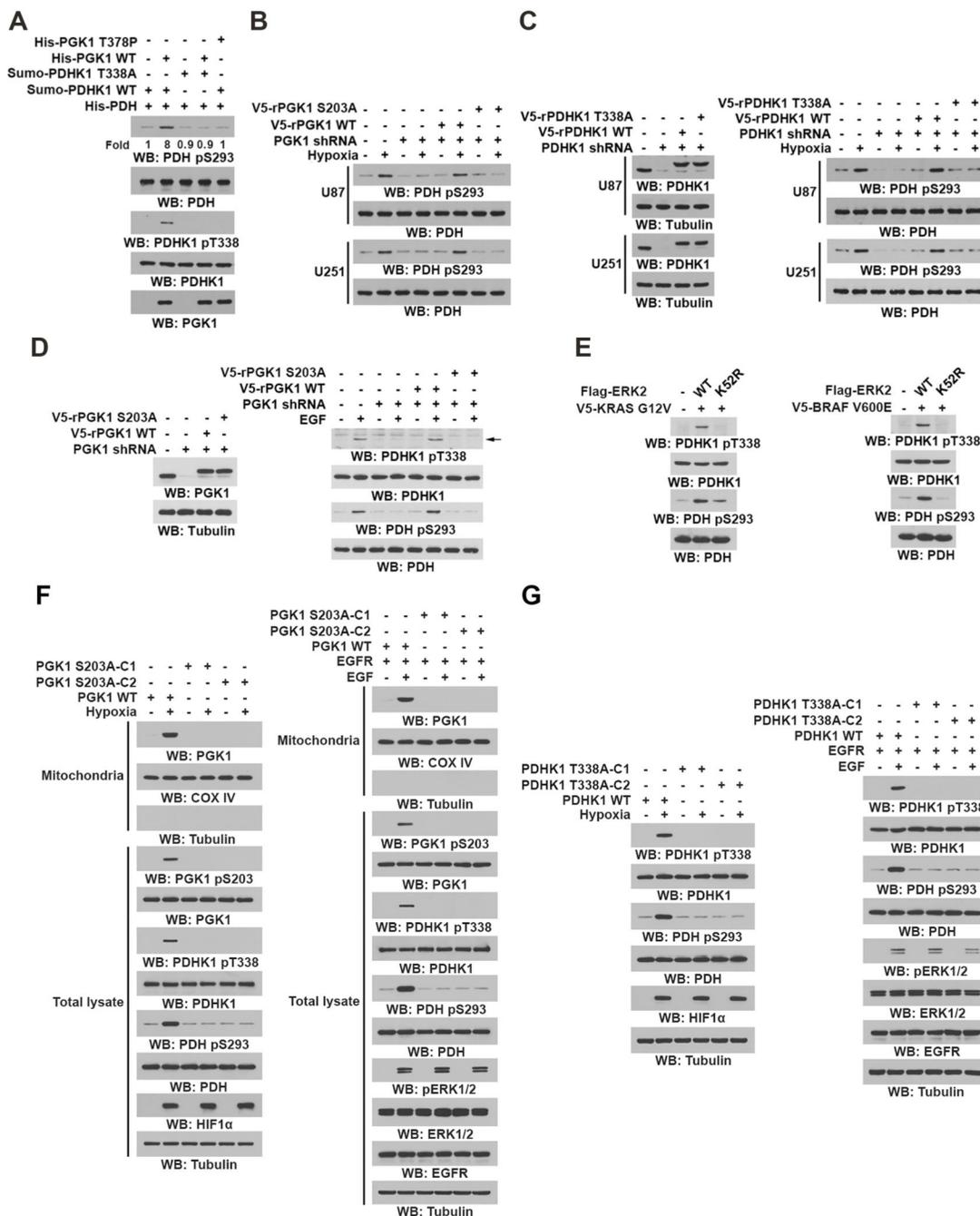
Figure 5. PDHK1 Phosphorylation by PGK1 Activates PDHK1

Immunoblotting analyses were performed with the indicated antibodies.

(A) Bacterially purified His-PDH (E1α) with purified WT PDHK1 or PDHK1 T338A was mixed with purified WT PGK1 or PGK1 T378P. In vitro phosphorylation analyses were performed.

(B, C) U87 and U251 cells expressing PGK1 shRNA (B) or PDHK1 shRNA (C) with or without reconstituted expression of the indicated proteins were stimulated with or without hypoxia for 6 h.

(D) U87/EGFR cells expressing PGK1 shRNA and with or without reconstituted expression of WT rPGK1 or rPGK1 S203A were stimulated with or without EGF (100 ng/ml) for 6 h.

(E) BxPC-3 cells were stably transfected with or without vectors expressing V5-KRAS G12V and the indicated Flag-ERK2 proteins (left panel). CHL1 cells were stably transfected with or without vectors expressing V5-BRAF V600E and the indicated Flag-ERK2 proteins (right panel).

(F, G) Parental U87 cells and the indicated clones of U87 cells with PGK1 S203A (F) or PDHK1 T338A (G) knock-in were stimulated with or without hypoxia (left panel) or EGF (100 ng/ml) (right panel) for 6 h. Mitochondrial fractions and total cell lysates were prepared.
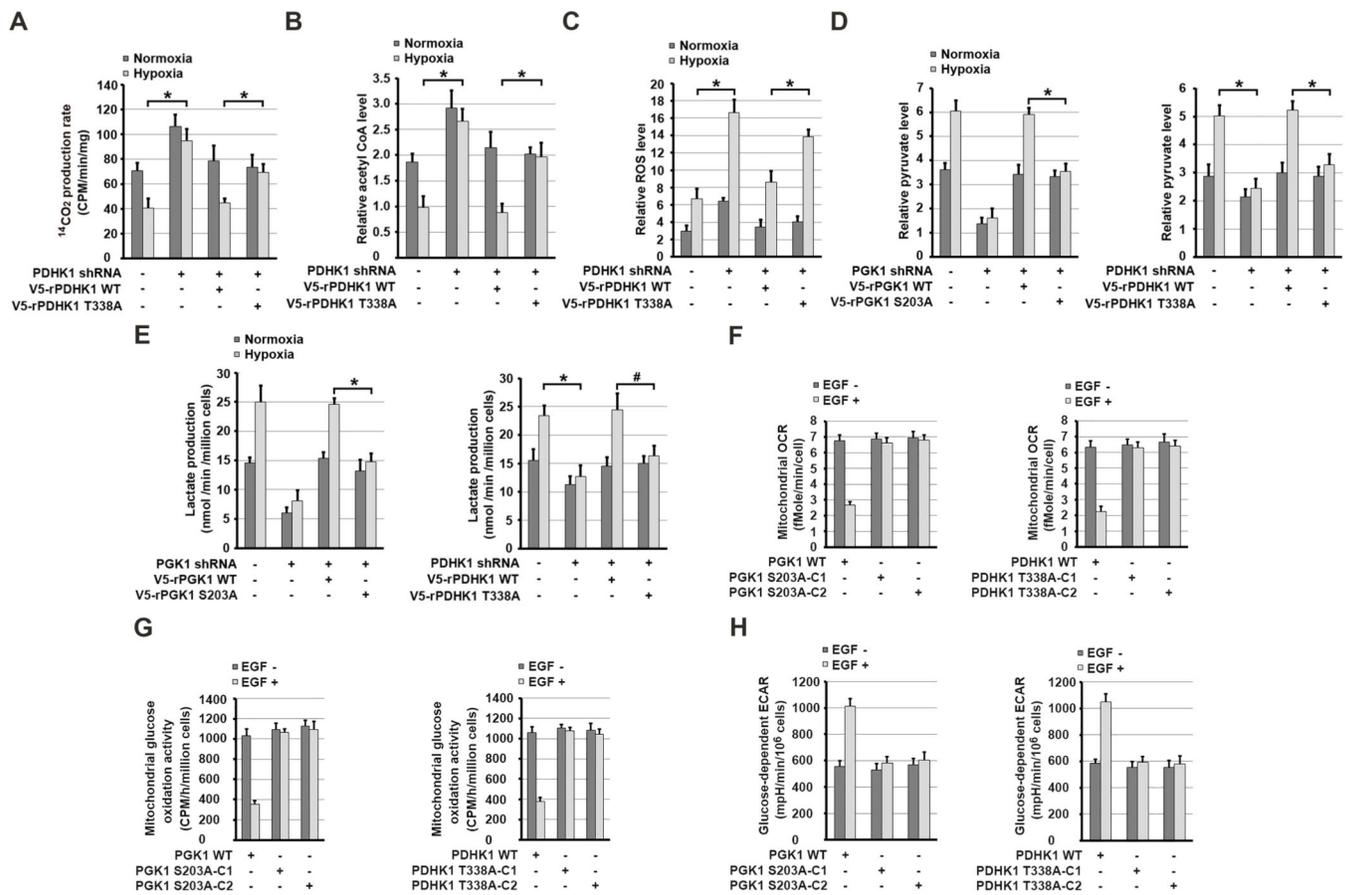
See also Figure S4.

Figure 6. PGK1-Mediated PDHK1 Phosphorylation Inhibits Mitochondrial Pyruvate Metabolism, Induces Hypoxia-Induced ROS Production, and Promotes Glycolysis

(A–H) Data represent the means ± SD of three independent experiments. *$p < 0.01$, #$p < 0.05$.

(A, B) U87 cells expressing PDHK1 shRNA with or without reconstituted expression of WT rPDHK1 or rPDHK1 T338A were stimulated with or without hypoxia for 6 h. Mitochondrial fractions of the cells were prepared and activity of PDH complex–mediated conversion of ^{14}C-pyruvate into ^{14}C-CO_2 was measured (A). Levels of mitochondrial acetyl-CoA were measured (B).

(C) U87 cells expressing PDHK1 shRNA with or without reconstituted expression of the indicated proteins were stimulated with or without hypoxia for 24 h. Levels of mitochondrial ROS were measured.

(D, E) U87 cells expressing PGK1 shRNA (left panel) or PDHK1 shRNA (right panel) with or without reconstituted expression of the indicated proteins were cultured in no-serum DMEM during hypoxia for 6 h. Levels of cytosolic pyruvate level were measured (D). The media were collected for analysis of lactate production (E).

(F and H) Serum-starved parental U87 cells and the indicated clones of U87 cells with PGK1 S203A (left panel) or PDHK1 T338A (right panel) knock-in were treated with or without EGF (100 ng/ml) for 6 h. The glucose-dependent mitochondrial OCR (F) and ECAR (H) in these cells were measured.

(G) Serum-starved parental U87 cells and the indicated clones of U87 cells with PGK1 S203A (left panel) or PDHK1 T338A (right panel) knock-in were treated with or without EGF (100 ng/ml) for 6 h and then incubated with 5 mM glucose spiked with 0.001 mM U-^{14}C glucose, 1-^{14}C glucose, or 6-^{14}C glucose for 2 h. The radioactivity levels of the cells were normalized according to cell number.
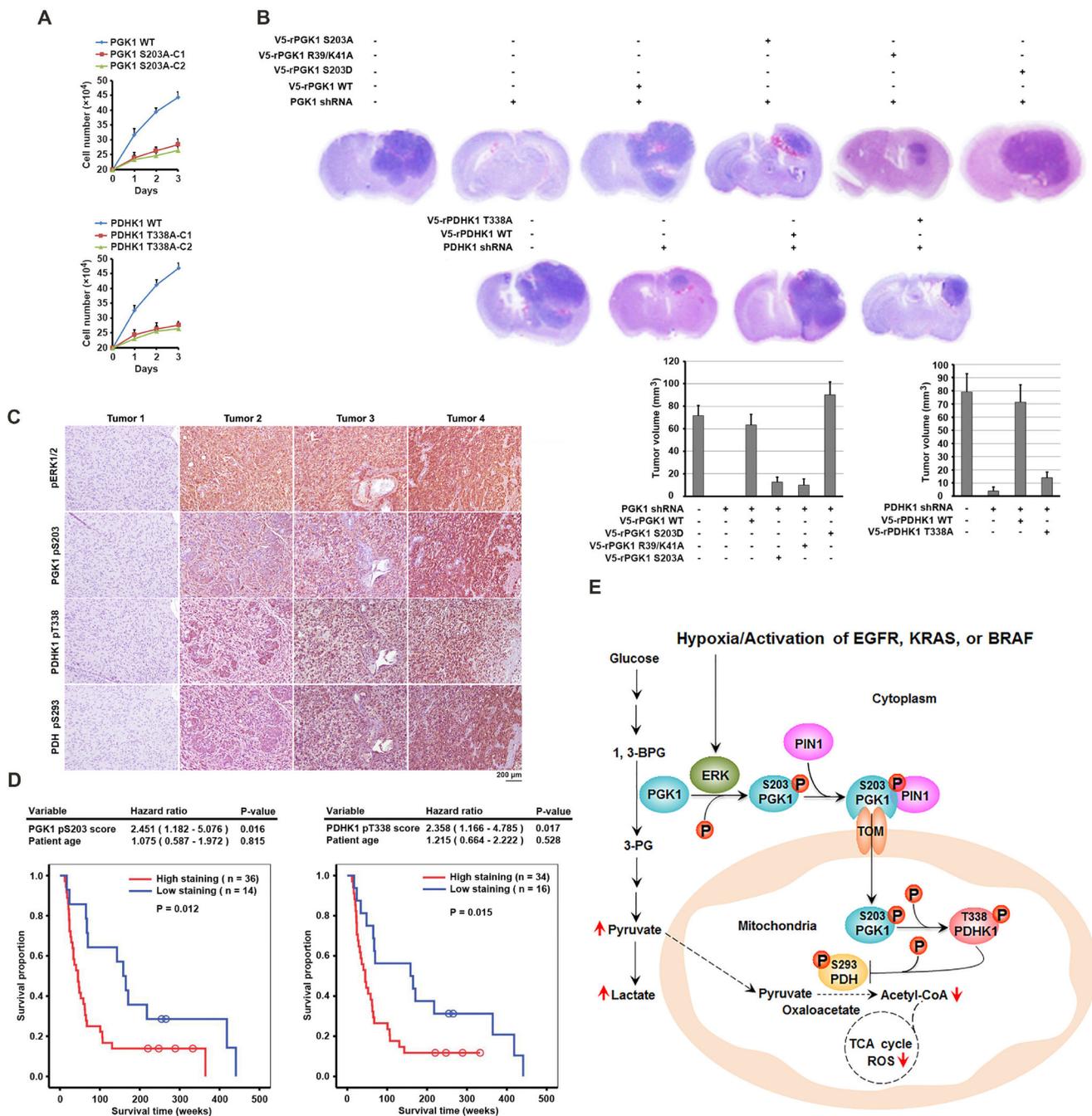
See also Figure S5.

Figure 7. Mitochondrial PGK1-Dependent PDHK1 Phosphorylation Promotes Cell Proliferation and Brain Tumorigenesis and Indicates a Poor Prognosis in GBM Patients

(A) Parental U87 cells (2×10^5) and the indicated clones of U87 cells with PGK1 S203A (upper panel) or PDHK1 T338A (lower panel) knock-in were plated for 3 days under hypoxic conditions. The cells were then collected and counted. The data are presented as the means ± SD from three independent experiments.

(B) U87 cells with or without PGK1 shRNA or PDHK1 shRNA expression and with or without reconstituted expression of the indicated proteins were intracranially injected into

athymic nude mice. H&E-stained coronal brain sections show representative tumor xenografts. Tumor volume was calculated.

(C) IHC staining with phospho-ERK1/2, PGK1 pS203, PDHK1 pT338, and PDH pS293 antibodies was performed on 50 human primary GBM specimens. Representative photos of four tumors are shown.

(D) The survival time for 50 patients with low (1–4 staining scores, blue curve) versus high (4.1–8 staining scores, red curve) phosphorylation levels of PGK1 S203 (low, 14 patients; high, 36 patients) and PDHK1 T338 (low, 16 patients; high, 34 patients) were compared. The table shows the multivariate analysis results after adjustment for patient age, indicating the significance level of the association of PGK1 S203 ($p = 0.016$) and PDHK1 T338 ($p = 0.017$) phosphorylation with patient survival. Empty circles represent censored data from patients alive at last clinical follow-up.

(E) A Mechanism of Mitochondrial PGK1-Coordinated Glycolysis and TCA Cycle in Tumorigenesis. Broken arrows: inhibited directions or reactions.

See also Figures S6, S7.